Cytochrome c Can Form a Well-Defined Binding Pocket for Hydrocarbons

Levi J. McClelland,[†,‡,§] Harmen B. B. Steele,[†,§] Frank G. Whitby,[∥] Tung-Chung Mou,[‡,§] David Holley,[§] J. B. Alexander Ross,[†,§] Stephen R. Sprang,[‡,§] and Bruce E. Bowler*,[†,§]

[†]Department of Chemistry & Biochemistry, University of Montana, Missoula, Montana 59812, United States
[‡]Division of Biological Sciences, University of Montana, Missoula, Montana 59812, United States
[§]Center for Biomolecular Structure & Dynamics, University of Montana, Missoula, Montana 59812, United States
[∥]Department of Biochemistry, University of Utah School of Medicine, Salt Lake City, Utah 84112, United States

S *Supporting Information*

ABSTRACT: Cytochrome c can acquire peroxidase activity when it binds to cardiolipin in mitochondrial membranes. The resulting oxygenation of cardiolipin by cytochrome c provides an early signal for the onset of apoptosis. The structure of this enzyme−substrate complex is a matter of considerable debate. We present three structures at 1.7−2.0 Å resolution of a domain-swapped dimer of yeast iso-1-cytochrome c with the detergents, CYMAL-5, CYMAL-6, and ω-undecylenyl-β-D-maltopyranoside, bound in a channel that places the hydrocarbon moieties of these detergents next to the heme. The heme is poised for peroxidase activity with water bound in place of Met80, which serves as the axial heme ligand when cytochrome c functions as an electron carrier. The hydroxyl group of Tyr67 sits 3.6−4.0 Å from the nearest carbon of the detergents, positioned to act as a relay in radical abstraction during peroxidase activity. Docking studies with linoleic acid, the most common fatty acid component of cardiolipin, show that C11 of linoleic acid can sit adjacent to Tyr67 and the heme, consistent with the oxygenation pattern observed in lipidomics studies. The well-defined hydrocarbon binding pocket provides atomic resolution evidence for the extended lipid anchorage model for cytochrome c/cardiolipin binding. Dimer dissociation/association kinetics for yeast versus equine cytochrome c indicate that formation of mammalian cytochrome c dimers in vivo would require catalysis. However, the dimer structure shows that only a modest deformation of monomeric cytochrome c would suffice to form the hydrocarbon binding site occupied by these detergents.
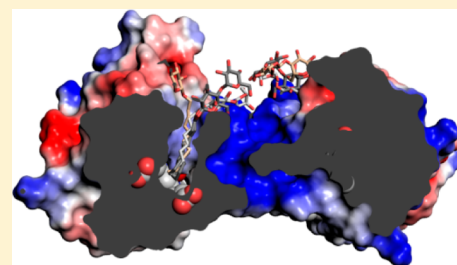
INTRODUCTION

Cytochrome c (Cytc) is well-known for its role in oxidative phosphorylation where its transfers electrons from complex III to complex IV.[1] More recently, Cytc has emerged as a critical mediator of the intrinsic pathway of apoptosis.[2−4] Not surprisingly given its involvement in two key pathways, the function of Cytc is regulated by phosphorylation.[5] Its function also appears to be affected by nitration under conditions of oxidative stress.[6] When associated with the negatively charged phospholipid, cardiolipin (CL), Cytc gains peroxidase activity.[3,4,7,8] Cytc mediated oxidization of the hydrocarbon chains of CL generates an early signal in the intrinsic pathway of apoptosis,[8] and may contribute to mitochondrial membrane permeabilization.[9] The specificity of CL oxidation indicates the existence of a well-defined hydrocarbon binding site.[10,11] Despite considerable effort, an atomic resolution structure of the Cytc hydrocarbon binding site has been lacking.[6] Here, we present three X-ray crystal structures at 1.7 to 2.0 Å resolution showing a well-defined binding pocket for the hydrocarbon chains of three different detergent molecules. The binding pocket holds the hydrocarbon chain of the detergents near an iron coordination site on the heme occupied by a water

molecule and thus could represent a resting state for peroxidase activity.

Binding of Cytc to CL is complex, and there is considerable debate in the literature about the nature of this interaction. However, four binding sites for CL, sites A, C, L, and N, on the surface of Cytc are most commonly discussed in the literature.[12−18] Site A (anionic binding site) is generally described as being primarily mediated by electrostatic interactions. Lysines 72, 73, 86, and 87 located in or near Ω-loop D (residues 70−85), which provides the Met80 heme ligand, are postulated to be the primary determinants of site A.[12,15−17] Site L is also mediated by a cluster of positively charged residues (Lys22, Lys 27, His33, and Lys87) located mainly on the opposite face of Cytc from site A. Thus, in conjunction with site A, site L can bridge membrane surfaces causing membrane fusion.[18] Binding at this site disappears above pH 7.5 due to deprotonation of site L residues. Site N (novel site), identified via chemical shift perturbation (^{15}N-^{1}H-HSQC) upon titration of CL into Cytc encapsulated in reverse micelles, encompasses residues Phe36, Gly37, Thr58, Trp59,

and Lys60, and thus also likely involves a component of electrostatic binding.[14] Site C (cardiolipin site) is a hydrophobic binding site and thus is most relevant to the current study. Binding data for site C suggest that one or more of the fatty acyl chains of CL rotates out of the membrane and inserts into a hydrophobic channel in Cyt*c*.[16,19−21] This mode of protein/membrane binding is referred to as an extended lipid anchorage.[16,20,22−24] Site C also requires protonation of a CL phosphate near physiological pH, permitting hydrogen bonding to Asn52.[15,16] Despite concurrent work which supported protonation of a CL phosphate in this pH regime,[25] recent studies question whether a CL phosphate ionizes near physiological pH.[26,27] Furthermore, the reverse micelle study, which identified site N, did not detect evidence for a CL binding site near Asn52.[14] Discrepancies in the magnitudes of binding constants for sites A and C also exist in the literature.[15,16,28−30] Thus, significant questions remain regarding the detailed nature of site C, the hydrophobic CL binding site.

Förster resonance energy transfer (FRET) studies on Cyt*c* labeled with fluorophores, together with other biophysical studies, indicate that Cyt*c* equilibrates between compact and partially unfolded extended conformers when bound to CL-containing liposomes.[13,28−33] There is evidence that the compact state may even, in part, retain Met80 ligation.[29,33] By contrast, solid-state NMR studies indicate that Cyt*c* remains in a native-like conformer when bound to CL liposomes and does not interact intimately with the hydrocarbon chains of CL,[34] as required for the extended lipid anchorage.[16,20] The study of Cyt*c* in reverse micelles also indicated that Cyt*c* remains folded in the presence of CL with no evidence for insertion of the hydrocarbon into the hydrophobic core of Cyt*c*.[14] The extended conformer observed in FRET studies appears to have enhanced peroxidase activity and thus could mediate apoptotic peroxidase activity.[28] However, oxygenation of CL by Cyt*c* is specific, consistent with a well-defined substrate binding site.[10]

Given the vigorous debate surrounding the nature of the interaction of Cyt*c* with lipids, we have undertaken atomic resolution structural studies on the interaction of detergents with Cyt*c* to model Cyt*c*/lipid binding. Here, we present high resolution X-ray structures of a domain-swapped dimer of yeast iso-1-cytochrome *c* (iso-1-Cyt*c*) carrying a K72A mutation bound to three different detergents. The hydrocarbon chain of each detergent is bound in the same pocket, holding the hydrocarbon chain close to the heme. In two cases, the detergent headgroup is well-ordered providing detailed insight into hydrogen bonding partners on the surface of Cyt*c* which can stabilize lipid interactions with Cyt*c*.

■ RESULTS AND DISCUSSION

Overall Structure of the Iso-1-Cyt*c*/Detergent Complexes. In this work, we used the K72A variant of yeast iso-1-cytochrome *c* (henceforth referred to as WT* iso-1-Cyt*c*), which previously facilitated crystallization of an alternate conformer of Cyt*c* with the Met80 heme ligand expelled from the heme crevice and replaced by hydroxide.[35] Co-crystals of WT* iso-1-Cyt*c* with the detergents, CYMAL-5, CYMAL-6, and *ω*-undecylenyl-*β*-D-maltopyranoside, (*ω*-UDM, see Figure 1A) were obtained from concentrated solutions of $(NH_4)_2SO_4$. The cocrystals of WT* iso-1-Cyt*c* with CYMAL-5 diffracted to 1.7 Å resolution (Table S1), whereas the cocrystals with CYMAL-6 and *ω*-UDM diffracted to 2.0 Å resolution (Tables
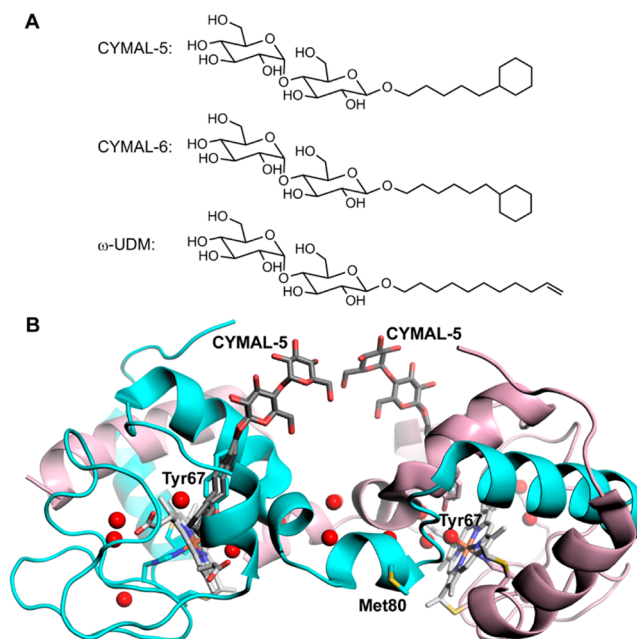

Figure 1. (A) Structures of the detergents used in this work. (B) Domain-swapped dimer structure of WT* iso-1-Cyt*c* in complex with CYMAL-5 (PDB code: 5KKE). There is one molecule in the unit cell (cyan). A symmetry-related molecule (mauve) is used to form the dimeric biological assembly. Met80, Tyr 67, the heme and the residues that attach the heme to the polypeptide, Cys14, Cys17, His18, are shown as stick models. Buried waters are shown as red spheres. CYMAL-5 (dark gray stick model) adopts two conformers with the cyclohexyl ring in a chair (55%) versus a boat (45%) conformation.

S2 and S3). Although all crystal trials were carried out with monomeric protein, WT* iso-1-Cyt*c* crystallized as a domain-swapped dimer in the presence of all three detergents (Figure 1B and Figures S1 and S2). The C-terminal *α*-helix of iso-1-Cyt*c* is swapped between the subunits of the dimer, which are related by 2-fold symmetry. In each case, two molecules of the detergent are bound to each dimer, incorporated into channels on each subunit of the dimer. The domain-swapped dimers with CYMAL-6 and *ω*-UDM as ligands overlay well with the CYMAL-5 domain-swapped dimer (backbone RMSD of 0.434 and 1.085 Å, respectively) indicating that these ligands occupy a robust hydrocarbon binding site (Figure S3). Even the positions of buried water molecules are well reproduced among the three structures (Figure S3).

There are minimal structural changes in the subunits of the dimer relative to monomeric iso-1-Cyt*c* (Figure S4). However, Ω-loop D (residues 70−85), which normally aligns Met80 for axial ligation to the heme, acts as a hinge loop between the two subunits. Water is bound to the heme in place of Met80 and ordered waters are found in place of the Met80 heme ligand (Figures 1 and 2 and Figure S4). Perturbation of Ω-loop D extends from residue 72 to residue 84. Starting with Leu85 at the end of Ω-loop D, the domain swapped C-terminal helix aligns well with its position in monomeric iso-1-Cyt*c* (Figure S4). Circular dichroism spectra in solution of monomeric WT* iso-1-Cyt*c* and dimeric WT* iso-1-Cyt*c* without detergent bound (apo-dimer, prepared by treatment with ethanol followed by size exclusion chromatography,[36] see Supporting Methods) are similar (Figure S5), consistent with the generally good alignment of monomeric WT* iso-1-Cyt*c* with the dimer subunit.
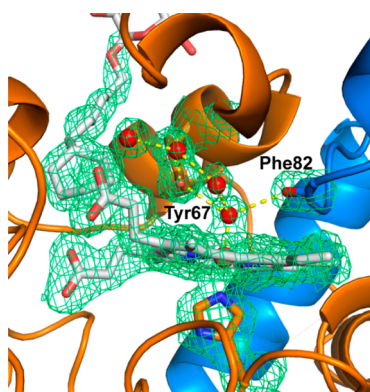
Figure 2. Close-up of the heme of the WT* iso-1-Cyt*c* domain-swapped dimer with CYMAL-6 as the ligand (PDB code: 5T7H). A Sigma-A weighted $2|F_o|−|F_c|$ electron density map contoured at 1.2σ (green mesh) for the water network (red spheres), the heme, His18, Tyr67, the carbonyl of Phe82 and CYMAL-6 (gray sticks) for the subunit formed with chain C (orange), and the C-terminal helix of chain B (blue).

Comparison with the Domain-Swapped Dimer of Equine Cyt*c*. The structure of a domain-swapped dimer of equine Cyt*c* has been reported.[37] It is similar to the WT* iso-1-Cyt*c* dimers reported here, but has no ligand bound (Figure S6). In both the yeast and the equine dimers, Ω-loop D acts as the hinge loop. However, the hinge loop is shorter in the equine dimer comprising only residues 78−83. The substrate binding pocket for the detergent molecules may require this more extended hinge loop. However, the observed differences may simply reflect the inherent flexibility of the hinge loop.[37−40] The B-factors in one subunit of the ω-UDM domain-swapped dimer are much higher than in the other, consistent with the flexibility of the hinge loop in the context of sparse crystal contacts (Table S4 and Figure S7).

Absorbance spectra in solution indicate that apo-dimer formation does not substantially perturb the heme environment relative to monomeric WT* iso-1-Cyt*c* (Figure S8A). The Soret absorbance band of the dimer (Figure S8B) is shifted 2

nm to shorter wavelength as for the equine Cyt*c* dimer.[37,41] Similar to the equine dimer,[37,41] the 695 nm band, corresponding to Met80-heme coordination,[42] is less intense in the iso-1-Cyt*c* apo-dimer but has not completely disappeared (Figure S8C). A possible explanation for this observation is that, in the absence of bound hydrocarbon, one of the swapped C-terminal helices can detach from its subunit allowing Met80 from the hinge loop to rebind to its original heme. This structure would be similar to the intermediate necessary for formation of a runaway domain-swap.[43]

Hydrocarbon Binding Pocket. Residues adjacent to the detergent binding pocket of the dimeric Cyt*c* complex undergo small, but significant, structural rearrangements relative to monomeric iso-1-Cyt*c* (Figure S4B, RMSD up to 3 Å). These structural perturbations extend from Ser40, which, with the heme, lies at the bottom of the hydrocarbon binding cavity, to Tyr74, which forms one wall of the binding pocket. Residues in the short 50s helix (residues 50−55), and the 60s helix also flank the binding pocket (Figure 3A). The heme and the aromatic residues, Tyr48, Tyr67, and Trp59 all contact the hydrocarbon chains. The position of the binding pocket corresponds surprisingly well to the left channel (residues 52−74) of hydrophobic residues defined in the first X-ray crystal structure of horse Cyt*c*.[19] For the straight chain hydrocarbon of ω-UDM, the 50s helix moves toward the heme, filling space that is occupied by the cyclohexyl rings of the CYMAL-5 and CYMAL-6 detergents. This movement is coupled to a shift in the position of Asn52 from a fully surface exposed position to one in which it is hydrogen bonded to a heme propionate through a bridging water (Figure S9). Thus, our results indicate that Asn52 is involved in forming the binding site for hydrocarbons in the extended lipid anchorage, although not as originally envisioned for site C.

A considerable number of structures exist in the protein data bank, which have either CYMAL-5 or CYMAL-6 bound to a protein. For CYMAL-6, most of these structures are of SHV β-lactamase variants with two molecules of CYMAL-6 bound in a surface crevice between helices 10 and 11, which is lined with aliphatic residues.[45,46] For CYMAL-5, most of the structures are
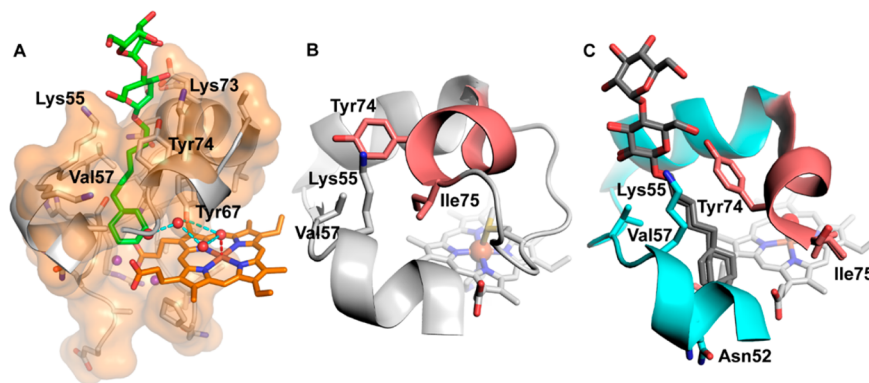

Figure 3. Formation of the hydrocarbon binding pocket. (A) View showing the water network (red spheres) between CYMAL-6 (green stick model) and the heme group. Residues 30−44 and 51−74 of chain C are shown as gray sticks with a transparent orange van der Waals surface. Residues lining the opening of the CYMAL-6 binding site are labeled. Two buried waters on the His18 side of the heme are shown as purple spheres. The hydrogen bonds, shown as cyan dashed lines, range from 2.70 to 3.09 Å. The bond from the heme iron to water is shown as a red dashed line. (B) Residues 50 to 84 of the monomer structure of iso-1-Cyt*c* (light gray, PDB code: 2YCC[44]). The heme and its ligands, His18 and Met80, are shown as stick models. (C) Residues 50 to 75 of the WT* iso-1-Cyt*c* dimer with CYMAL-5 (PDB code: 5KKE, cyan) bound. Heme is shown as a stick model. CYMAL-5 (dark gray) is shown as a stick model. The 70s helix (residues 70−75), which rearranges upon detergent binding, is shown in salmon in panels B and C. The residues that move to form the hydrocarbon binding pocket, Asn52 (visible only in C), Lys55, Val57, Tyr74, and Ile75, are labeled and shown as stick models in panels B and C.
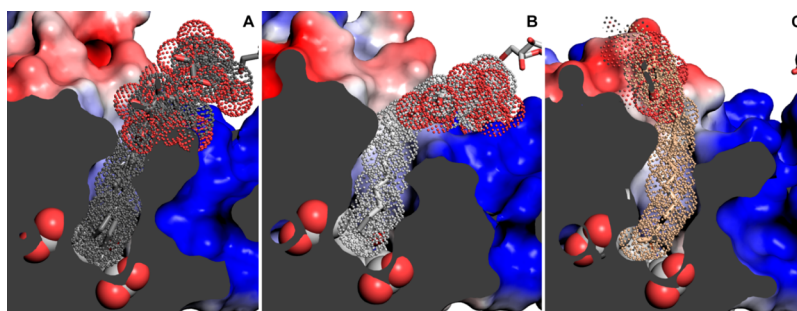
Figure 4. Close-up cutaway view of the hydrocarbon binding cavity. A dotted surface at the van der Waals radius (carbon in dark gray, light gray and beige for A, B, and C, respectively; oxygen, red) is superimposed on the (A) CYMAL-5, (B) CYMAL-6, and (C) ω-UDM structures in the cavity. Blue corresponds to a positive charge surface, white is a neutral charge surface, and red is a negative charge surface. Heme is shown as a space-filling model (red spheres protruding through the gray surface are the oxygen atoms of the heme propionates.

with cytochrome P450 2B4 variants.[47,48] In one instance structures of both the empty and occupied binding sites are available.[48] As with our iso-1-Cytc detergent bound structures, numerous small side chain and backbone adjustments occur when CYMAL-5 binds to cytochrome P450 2B4, relative to the structure without CYMAL-5 bound. As in our structure, a number of aromatic side chains line the binding cavity. Intriguingly, detergent binding appears to enhance the dynamics of cytochrome P450 2B4, which could allow for more efficient substrate exchange.[48] For fatty acid binding proteins, the binding pockets are also lined with aromatic and aliphatic residues[49−52] and in one case a domain-swapped dimer is observed.[50]

In monomeric iso-1-Cytc, Tyr74 occupies part of the hydrocarbon binding pocket in the dimer (Figure 3B). The significant shifts in the positions of Asn52, Tyr74, and Ile75 in the dimer, coupled to smaller shifts in the positions of Lys55 and Val57, create the hydrocarbon binding pocket in the domain-swapped dimer of WT* iso-1-Cytc (Figure 3B versus Figure 3C). It is perhaps not surprising that the hydrocarbon binding site is located in this region of iso-1-Cytc. As noted above, it corresponds well to the left channel (residues 52−74) of hydrophobic residues defined in the first X-ray crystal structure of horse Cytc.[19] The residues that move to form the binding pocket also correspond to the least stable infrared (residues 40 to 57) and red (residues 70−85) substructures of Cytc.[53−55]

The rearrangements necessary to accommodate the hydrocarbon chains only modestly affect the tertiary structure of Cytc (see Figure S4) indicating that this binding cavity might be accessible in monomeric Cytc and may simply be more stable in the dimer. The hydrocarbon chain of each of the three detergents fits tightly into the binding pocket of dimeric WT* iso-1-Cytc, which is a well-defined channel extending from the surface of the protein to the edge of the heme (Figure 4). This channel differs from the potential binding pocket noted in a recent structure of an alkaline conformer of iso-1-Cytc, which is a crevice in the surface of the protein that sits above the heme rather than a channel to the heme.[56]

There are also openings in the solvent-accessible surface of each subunit of our iso-1-Cytc dimer structures that would allow reactive oxygen species, necessary for peroxidase activity, to enter the substrate binding site and bind to the heme iron. These include a crevice framed by Ala51, Lys54, Lys55, and Tyr74, which provides access to the bottom of the hydrocarbon binding pocket (Figure S10A). A small opening bordered by

Ser40, Gly41, Asn52, and Asn56 is also present in some, but not all, cases (Figure S10B).

Position of the Detergent Head Groups on the Surface of the Dimer. The electrostatic surface in Figure 5A illustrates that the entrance to the binding pocket would position the negatively charged headgroup of CL adjacent to a positive patch on the dimer surface. Lys73, a residue that has been implicated in site A binding, is also positioned at the channel entrance (Figure 3A).
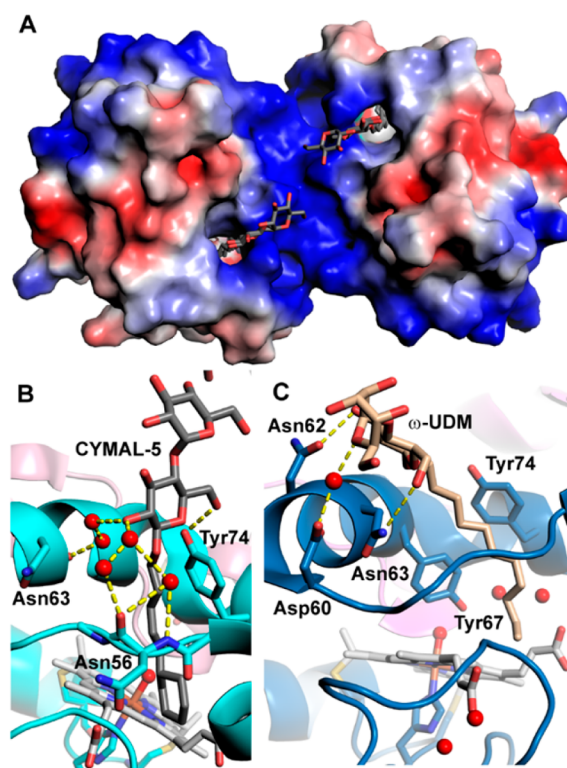

Figure 5. Head group interactions with the surface of the domain-swapped dimer of iso-1-Cytc. (A) Electrostatic potential surface of the domain-swapped dimer showing CYMAL-5 emerging from the binding cavity (PDB code: 5KKE). (B) Hydrogen bonding interactions of CYMAL-5 with residues at the surface of the domain-swapped dimer (PDB code: 5KKE). (C) Hydrogen bonding interactions of ω-UDM with residues at the surface of the domain-swapped dimer (PDB code: 5KLU). Waters are shown as red spheres and hydrogen bonds are shown as yellow dashed lines.

The electron density of the alkyl chain of CYMAL-6 is well-defined (Figure 2). However, the maltose headgroup of CYMAL-6, which projects into solvent (Figure S1), is associated with weak and discontinuous electron density indicating that it is disordered. By contrast, the maltose head groups of CYMAL-5 and ω-UDM have well-defined electron density (Figure S11), allowing clear assessment of the nature of the interaction of their head groups with the surface of the domain-swapped dimer. Because the maltose headgroup carries no charge, its interactions are not governed by the electrostatics of the surface of the dimer. The headgroup of CYMAL-5 sits over a positive electrostatic surface (Figures 4A and 5A), whereas that of ω-UDM interacts with a more negatively charged portion of the surface of the domain-swapped dimer (Figure 4C). Extensive hydrogen bonding interactions, some of which are mediated by ordered waters, anchor the headgroups of CYMAL-5 (Figure 5B) and ω-UDM (Figure 5C) to the surface of the domain-swapped dimer. The maltose headgroup of CYMAL-5 is hydrogen bonded to the hydroxyl group of Tyr74, and to the main chain carbonyl of Asn63 and the main chain heteroatoms of Asn56 via bridging waters. The maltose headgroup of ω-UDM interacts with the Asp60 (through a bridging water), Asn62, and Asn63 side chains at the N-terminal end of the 60s helix. Thus, a wealth of hydrogen bonding groups, which could interact with the headgroup of a lipid like CL, surrounds the opening to the hydrocarbon binding cavity.

Docking of Linoleic Acid into the Hydrocarbon Binding Pocket. The hydrocarbon chains of the three detergents cocrystallized with WT* iso-1-Cyt*c* contain 11 to 12 carbons. The straight chain hydrocarbon of ω-UDM is a C11 hydrocarbon, whereas the fatty acyl chains of CL range from C16 to C22.[10] The most common fatty acid in CL, linoleic acid,[57] is a C18 hydrocarbon. It has C9 and C12 *cis* double bonds, so the C11 hydrogens are expected to be particularly susceptible to radical abstraction followed by oxygenation because the radical produced is stabilized by delocalization across five carbons (Figure 6).

In all three of our structures, two to three water molecules form a hydrogen bond network with Tyr67 and the water bound to the heme iron. Displacement of these waters could allow accommodation of a larger hydrocarbon chain. To test whether longer hydrocarbon chains can fit into the binding cavity, we docked linoleic acid into the binding cavity of the WT* iso-1-Cyt*c* dimer (CYMAL-6 structure). In the docking procedure, all waters were removed, except for the water bound to the heme iron. C11 of linoleic was constrained to be within 5 Å of the Fe atom of the heme. The carboxylate of linoleic acid was constrained to be within 10 Å of Tyr74, which is near the juncture of the hydrocarbon chain and the headgroup of both CYMAL-5 and CYMAL-6. Docking identified three similar poses for linoleic acid with strong positive Chemscores[58] ranging from 34 to 39, indicating viable binding poses. The hydrocarbon chain of linoleic acid near the carboxylic acid group is in a similar position to the hexamethylene chain of CYMAL-6 (Figures 6 and S12). The C11 carbon of linoleic acid is on average 3.8 ± 0.6 Å from the water bound to the heme iron. The hydrocarbon chain of linoleic acid then reverses direction, occupying space vacated by the water molecules in the binding cavity. In structures of fatty acid binding proteins, it is typical that linoleic and other long chain fatty acids adopt U-shaped structures as observed in our docking poses.[49−52] The terminal methyl group of linoleic acid is located near the
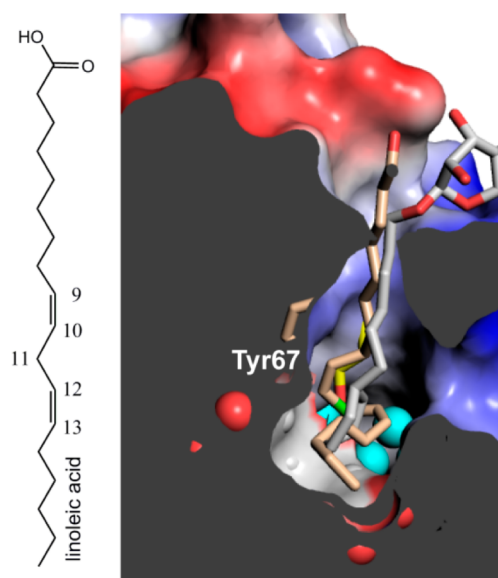

Figure 6. Docking of linoleic acid (beige sticks) into the binding cavity of the CYMAL-6/WT* iso-1-Cyt*c* structure (PDB code: 5T7H). CYMAL-6 is shown in light gray sticks. Buried waters and the water bound to the heme iron are shown as cyan spheres. The position of Tyr67 in the CYMAL-6 structure is shown with yellow sticks and in the linoleic acid docked structure with beige sticks (partially protruding through gray surface). C11 of linoleic acid is colored green. The Chemscore of this pose is 34. The structure of linoleic acid is shown on the left.

cyclohexyl ring of CYMAL-6 in all three poses (Figures 6 and S12). The poses also required movement of Tyr67 (Figures 6 and S12). The distance from C11 of linoleic acid to the hydroxyl group of Tyr67 is more variable. It is 3.5 Å from the hydroxyl group of Tyr67 in Figure 6, but this distance is ~7.5 Å in the two poses in Figure S12.

Insights into Peroxidase Mechanism from the Hydrocarbon Binding Site. When Cyt*c* functions as a peroxidase, hydrogen peroxide first interacts with the heme to form Compound I, followed by conversion to Compound II and a tyrosyl radical.[36,59,60] Tyr67 has been implicated in radical-driven hydrogen abstraction from CL during CL oxidation.[59] In the structure of the CYMAL-6 complex, for the four subunits in the asymmetric unit, the average distance from the hydroxyl group of Tyr67 to the closest carbon on the cyclohexyl ring is 3.6 ± 0.2 Å (Figure 2 and Figure 3A). Similarly, the C9 carbon (next to the terminal double bond) of the C11 hydrocarbon chain of ω-UDM is 4.0 Å from the hydroxyl of Tyr67 and the closest carbon of the cyclohexyl ring of CYMAL-5 is 3.9 Å from the hydroxyl group of Tyr67. Thus, the hydrocarbon binding channel of the domain-swapped dimer of WT* iso-1-Cyt*c* positions the hydrocarbon chain of all three detergents for hydrogen abstraction by Try67, consistent with existing biochemical data.[59]

Docking of linoleic acid into the hydrocarbon binding pocket of the domain-swapped dimer of iso-1-Cyt*c* also shows that it is feasible to accommodate the C11 carbon within close proximity of both the hydroxyl group of Tyr67 and of the oxygen atom of water bound to the heme iron. Lipidomics studies show that oxygenation of linoleic acid in CL catalyzed by Cyt*c* occurs primarily between carbons 9 and 13,[10,11] consistent with hydrogen abstraction from C11 located between the two double bonds of linoleic acid (Figure 6). Thus, the observed

hydrocarbon binding site can feasibly explain the observed oxygenation pattern of linoleic acid.

Stability of Dimeric Cyt*c*. An increasing number of domain-swapped dimers has been characterized and in some cases these dimers are believed to play a physiological role in protein function.[61] The equine Cyt*c* dimer has enhanced peroxidase activity relative to monomeric equine Cyt*c*, which has led to the suggestion that the dimer might mediate peroxidase activity early in apoptosis.[36] Although, direct evidence for domain-swapped dimers of mitochondrial Cyt*c* in vivo is lacking, recent work has shown that *Hydrogenobacter thermophilus* cytochrome c_{552} can form domain-swapped dimers and oligomers in vivo (in the soluble fraction) when expressed in *Escherichia coli*.[62] However, harsh conditions, treatment with ethanol or detergent, are required to form the dimer in vitro.[37−40] Only qualitative data on the stability of the domain-swapped dimer of Cyt*c* is available.[37] Thus, we measured the kinetic stability of both equine Cyt*c* and WT* iso-1-Cyt*c* apo-dimers prepared by treatment with ethanol[37−40] (Figures S13 and S14). WT* iso-1-Cyt*c* dimers dissociate at measurable rates in the 10 to 30 °C range, whereas equine Cyt*c* dimer dissociation is measurable from 40 to 60 °C (Table 1). The kinetically more stable equine Cyt*c* dimer has a lifetime of 7.4 days at 40 °C.

The curvature in the Eyring plot for the WT* iso-1-Cyt*c* dimer (Figure 7) is consistent with a significant change in the

Table 1. Rate Constants for Dimer to Monomer Conversion, k_{DM}, for WT* iso-1-Cyt*c* and Equine Cyt*c* Dimers

Yeast iso-1-Cyt*c*		Equine Cyt*c*	
T (°C)	k_{DM} (s^{-1})^a	T (°C)	k_{DM} (s^{-1})^a
30	$3.4 \pm 0.4 \times 10^{-3}$	60	$1.0 \pm 0.2 \times 10^{-2}$
25	$5.5 \pm 0.3 \times 10^{-4}$	55	$8 \pm 2 \times 10^{-4}$
20	$6.1 \pm 0.5 \times 10^{-5}$	50	$9 \pm 3 \times 10^{-5}$
15	$1.6 \pm 0.4 \times 10^{-5}$	45	$1.5 \pm 0.3 \times 10^{-5}$
10	$6.5 \pm 0.7 \times 10^{-6}$	40	$1.6 \pm 0.1 \times 10^{-6}$

^{a}Parameters are the average and standard deviation of a minimum of three independent trials.
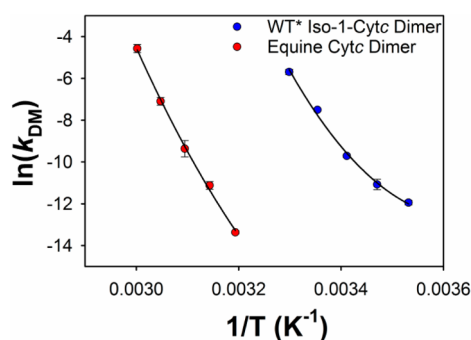

Figure 7. Erying plot for dimer dissociation rate constants, k_{DM}, of WT* iso-1-Cyt*c* and equine Cyt*c* dimers. The natural log of k_{DM} in units of s^{-1} is used for the plot. The solid curve is a fit to a form of the Eyring equation that accounts for $\Delta C_p^{\ddagger}$ (eq S1 in Supporting Methods). The reference temperature, T_o, was set to 298.15 K for both fits to eq S1. $\Delta H^{\ddagger}_{To} = 70 \pm 5$ kcal mol^{-1}, and $\Delta S^{\ddagger}_{To} = 0.16 \pm 0.02$ kcal mol^{-1} K^{-1} for dissociation of the yeast dimer and $\Delta H^{\ddagger}_{To} = 44 \pm 22$ kcal mol^{-1}, and $\Delta S^{\ddagger}_{To} = 0.06 \pm 0.07$ kcal mol^{-1} K^{-1} for dissociation of the equine dimer.

heat capacity, $\Delta C_p^{\ddagger}$, to attain the transition state for dimer dissociation. A fit of the WT* data in Figure 7 to eq S1 (Supporting Methods) yields $\Delta C_p^{\ddagger} = 3.0 \pm 0.8$ kcal mol^{-1} K^{-1}, which exceeds the ΔC_p of ~1.4 kcal mol^{-1} K^{-1} for thermal unfolding of monomeric yeast iso-1-Cyt*c* by 2-fold.[63,64] Thus, $\Delta C_p^{\ddagger}$ indicates that dimer dissociation requires full unfolding of both dimer subunits. The lower curvature in the equine data yields $\Delta C_p^{\ddagger} = 1.8 \pm 0.9$ kcal mol^{-1} K^{-1}, indicating that dimer dissociation requires significant, but possibly not complete, unfolding of the dimer subunits. Preparation of the equine Cyt*c* dimer in vitro requires refolding from a denatured[37,65] or molten globule state,[66] also consistent with the transition state for the monomer−dimer equilibrium being unfolded Cyt*c*. In a number of other instances, the transition state for the monomer−dimer equilibrium for domain-swapped dimers also appears to require full unfolding of the protein.[67,68] Mammalian Cyt*c* are considerably more stable than yeast iso-1-Cyt*c*.[69] If peroxidase activity of Cyt*c* is in part mediated by the domain-swapped dimer, the evolution of more stable mitochondrial Cyt*c* may be an adaption that allows tighter regulation of the peroxidase activity of Cyt*c* in mammals, at the onset of apoptosis, relative to yeast, which lacks a complete apoptotic pathway.[70]

WT* iso-1-Cyt*c* dimerizes on a time scale of months under conditions similar to those used for crystallization (Figure S15). The slower rate of dimer formation relative to dimer breakdown indicates that monomeric Cyt*c* is more stable than dimeric Cyt*c*. Thus, it seems that some form of catalysis, perhaps on a CL membrane surface, would be necessary to produce dimer in vivo. The observations that an extended conformer with the C-terminal helix of Cyt*c* unfolded can form on CL vesicles[28,31] and that sodium dodecyl sulfate can catalyze formation and breakdown of the domain-swapped dimer of Cyt*c*[37] suggest that such catalysis is feasible.

CONCLUSION

We have solved three structures of an iso-1-Cyt*c* C-terminal domain-swapped dimer each with a different detergent bound inside a conserved cavity. The binding cavity positions the hydrocarbon chain adjacent to Tyr67 and heme with an available coordination site. Both of these groups could catalyze peroxidation of CL.[36,59] Our structures also provide atomic resolution evidence for the proposed extended lipid anchorage model for Cyt*c*/CL interaction.[16,20] The hydrocarbon binding site, while observed in a domain-swapped dimer, could be achieved with relatively minor conformational adjustments to monomeric Cyt*c* (Figure 3B,C). Cyt*c*/CL binding studies indicate that Cyt*c*/membrane interactions are complex.[3,4,13,15,17,20,21,28−34] Thus, we cannot rule out other proposed CL/Cyt*c* binding modes with the current data.[13,28,29,33,34] However, the well-defined hydrocarbon binding site in our structure and docking studies of linoleic acid into the binding site are consistent with the binding site being able to lead to efficient abstraction of a hydrogen from C11 to produce the observed pattern of oxygenation of the linoleic acid component of CL by Cyt*c*.[10,11]

EXPERIMENTAL PROCEDURES

Protein Expression and Purification. Cyt*c* from equine heart was purchased from Sigma (C2506) and used without further purification. WT* iso-1-Cyt*c* was expressed from *E. coli* BL21(DE3) cells carrying the pRbs_BTR1 vector,[54] as described previously.[71] WT* iso-1-Cyt*c* has a K72A mutation to prevent K72 from acting as

an alkaline state ligand[72] and a C102S mutation to prevent disulfide dimerization during physical studies.[73] WT* iso-1-Cyt*c* was purified as previously described.[71,74,75] More detailed procedures are provided in Supporting Methods.

Crystallization, Structure Determination, and Refinement. A 2:2:1 mixture of oxidized WT* iso-1-Cyt*c* at 16−18 mg/mL in 75% aqueous ammonium sulfate, a reservoir solution of concentrated ammonium sulfate, 0.1 M Tris−HCl (pH 7.4−7.5) and detergent solution was crystallized at 20 °C by vapor diffusion from either hanging or sitting drops. Diffraction data were collected at the Stanford Synchrotron Radiation Lightsource or in-house with a Rigaku Micromax-007HF rotating anode source. The structures were solved by molecular replacement and refined to good R_{work} and R_{free} values at resolutions ranging from 1.70 to 2.00 Å. The coordinates and structure factors for the domain-swapped dimer of WT* iso-1-Cyt*c* complexed to CYMAL-5, CYMAL-6, and ω-UDM have been deposited at the Protein Data Bank (www.pdb.org) with ID codes, 5KKE, 5T7H, and 5KLU, respectively. A more complete description of crystallization, data collection, and refinement procedures may be found in Supporting Methods.

Dimer Dissociation Kinetics. The domain-swapped dimer of WT* iso-1-Cyt*c* was prepared by addition of ethanol to 80% (v/v). After lyophilization, WT* iso-1-Cyt*c* was resuspended in 50 mM potassium phosphate buffer, pH 7, at 4 °C. Equine Cyt*c* domain-swapped dimer was prepared using a literature procedure.[36] Both domain-swapped dimers were purified by size exclusion chromatography using a BioRad Enrich SEC-70 column and an AKTA-FPLC (GE Healthcare). Conversion of dimer to monomer was followed as a function of time by FPLC using the BioRad Enrich SEC-70 column. Samples were incubated in a fixed-temperature water bath, with the conversion of dimer to monomer quenched at a given time point by transferring an aliquot from the incubation solution to a micro-centrifuge tube that had been precooled on ice. Each aliquot was separated by FPLC at a temperature of 4 °C. The proportion of dimer and monomer at each time point was quantified from the chromatogram and used to extract k_{DM}. Additional details on experimental procedures are provided in Supporting Methods.

Docking of Linoleic Acid into the Hydrocarbon Binding Site. The yeast iso-1-Cyt*c*/CYMAL-6 crystal structure (PDB code: 5T7H) was used for docking. All crystallographic waters except the one bound to the heme iron were removed. A representation of linoleic acid was docked using GOLD suite 5.2.2[76] in Hermes 1.6.1 into the iso-1-Cyt*c*/CYMAL-6 domain-swapped dimer (molecules A and D with the CYMAL-6 ligand deleted) using CYMAL-6 as a reference ligand with a similarity constraint of 5. C11 of linoleic acid was restrained to be within 5 Å of the heme iron and the carboxylate of linoleic acid was constrained to be within 10 Å of Tyr74. For all docking runs, the side chains for N52, K55, N62, N63, E66, and Y67 were allowed to be flexible. The docked poses were scored using the Chemscore scoring function.[58] The resulting poses were then filtered for poses most consistent with biochemical data on the oxidation of CL and visualized with PyMol 1.7 (Schrödinger, LLC).

ASSOCIATED CONTENT

Ⓢ Supporting Information

The Supporting Information is available free of charge on the ACS Publications website at DOI: 10.1021/jacs.6b10745.

> Additional experimental procedures including crystallization procedures, X-ray crystallography data collection and refinement methods, spectral measurement procedures, and procedures for measuring dimer dissociation kinetics; additional tables including X-ray crystallography data collection and refinement parameters; additional figures including structures for the domain-swapped dimers with CYMAL-6 and ω-UDM bound, overlays of these two structures with the CYMAL-5 bound dimer, an overlay of a subunit of the domain-swapped dimer with CYMAL-6 bound and the monomeric structure of yeast

iso-1-cytochrome *c*, an overlay of the yeast domain-swapped dimer with the horse domain-swapped dimer, comparison of CD and absorbance spectra of the domain-swapped dimer with those for monomeric yeast iso-1-cytochrome *c*, a close-up view of an overlay of the heme ligation environment for the CYMAL-5 and ω-UDM bound domain-swapped dimer structures, additional linoleic acid docking poses, size exclusion chromatograms used to analyze dimer dissociation, and kinetic curves for dimer dissociation (PDF)

AUTHOR INFORMATION

Corresponding Author

*bruce.bowler@umontana.edu

ORCID Ⓞ

Bruce E. Bowler: 0000-0003-1543-2466

Notes

The authors declare no competing financial interest.

REFERENCES

(1) Dickerson, R. E.; Timkovich, R. In *The Enzymes*, 3rd ed.; Boyer, P. D., Ed.; Academic Press: New York, 1975; Vol. 11, p 397.

(2) Liu, X.; Kim, C. N.; Yang, J.; Jemmerson, R.; Wang, X. *Cell* **1996**, *86*, 147.

(3) Ow, Y. P.; Green, D. R.; Hao, Z.; Mak, T. W. *Nat. Rev. Mol. Cell Biol.* **2008**, *9*, 532.

(4) Kagan, V. E.; Bayir, H. A.; Belikova, N. A.; Kapralov, O.; Tyurina, Y. Y.; Tyurin, V. A.; Jiang, J.; Stoyanovsky, D. A.; Wipf, P.; Kochanek, P. M.; Greenberger, J. S.; Pitt, B.; Shvedova, A. A.; Borisenko, G. *Free Radical Biol. Med.* **2009**, *46*, 1439.

(5) Hütteman, M.; Doan, J. W.; Goustin, A.-S.; Sinkler, C.; Mahapatra, G.; Shay, J.; Liu, J.; Elbaz, H.; Aras, S.; Grossman, L. I.; Ding, Y.; Zielske, S. P.; Malek, M. H.; Sanderson, T. H.; Icksoo, L. In *Cytochromes b and c: biochemical properties, biological functions and electrochemical analysis*; Thom, R., Ed.; Nova Science Publishers: New York, NY, 2014; p 1.

(6) Hannibal, L.; Tomasina, F.; Capdevila, D. A.; Demicheli, V.; Tórtora, V.; Alvarez-Paggi, D.; Jemmerson, R.; Murgida, D. H.; Radi, R. *Biochemistry* **2016**, *55*, 407.

(7) Mugnol, K. C. U.; Ando, R. A.; Nagayasu, R. Y.; Faljoni-Alario, A.; Brochsztain, S.; Santos, P. S.; Nascimento, O. R.; Nantes, I. L. *Biophys. J.* **2008**, *94*, 4066.

(8) Kagan, V. E.; Tyurin, V. A.; Jiang, J.; Tyurina, Y. Y.; Ritov, V. B.; Amoscato, A. A.; Osipov, A. N.; Belikova, N. A.; Kapralov, A. A.; Kini, V.; Vlasova, I. I.; Zhao, Q.; Zou, M.; Di, P.; Svistunenko, D. A.; Kurnikov, I. V.; Borisenko, G. G. *Nat. Chem. Biol.* **2005**, *1*, 223.

(9) Firsov, A. M.; Kotova, E. A.; Korepanova, E. A.; Osipov, A. N.; Antonenko, Y. N. *Biochim. Biophys. Acta, Biomembr.* **2015**, *1848*, 767.

(10) Tyurina, Y. Y.; Domingues, R. M.; Tyurin, V. A.; Maciel, E.; Domingues, P.; Amoscato, A. A.; Bayir, H.; Kagan, V. E. *Chem. Phys. Lipids* **2014**, *179*, 3.

(11) Tyurin, V. A.; Tyurina, Y. Y.; Jung, M.-Y.; Tungekar, M. A.; Wasserloos, K. J.; Bayir, H.; Greenberger, J. S.; Kochanek, P. M.; Shvedova, A. A.; Pitt, B.; Kagan, V. E. *J. Chromatogr. B: Anal. Technol. Biomed. Life Sci.* **2009**, *877*, 2863.

(12) Kostrzewa, A.; Páli, T.; Froncisz, W.; Marsh, D. *Biochemistry* **2000**, *39*, 6066.

(13) Muenzner, J.; Pletneva, E. V. *Chem. Phys. Lipids* **2014**, *179*, 57.

(14) O'Brien, E. S.; Nucci, N. V.; Fuglestad, B.; Tommos, C.; Wand, A. J. *J. Biol. Chem.* **2015**, *290*, 30879.

(15) Rytömaa, M.; Kinnunen, P. K. J. *J. Biol. Chem.* **1994**, *269*, 1770.

(16) Rytömaa, M.; Kinnunen, P. K. J. *J. Biol. Chem.* **1995**, *270*, 3197.

(17) Kalanxhi, E.; Wallace, C. J. A. *Biochem. J.* **2007**, *407*, 179.

(18) Kawai, C.; Prado, F. M.; Nunes, G. L. C.; Di Mascio, P.; Carmona-Ribeiro, A. M.; Nantes, I. L. *J. Biol. Chem.* **2005**, *280*, 34709.

(19) Dickerson, R. E.; Takano, T.; Eisenberg, D.; Kallai, O. B.; Samson, L.; Cooper, A.; Margoliash, E. *J. Biol. Chem.* **1971**, *246*, 1511.

(20) Tuominen, A. K. J.; Wallace, C. J. A.; Kinnunen, P. K. J. *J. Biol. Chem.* **2002**, *277*, 8822.

(21) Sinibaldi, F.; Howes, B. D.; Piro, M. C.; Polticelli, F.; Bombelli, C.; Ferri, T.; Coletta, M.; Smulevich, G.; Santucci, R. *JBIC, J. Biol. Inorg. Chem.* **2010**, *15*, 689.

(22) Mahalka, A. K.; Kirkegaard, T.; Jukola, L. T. I.; Jäättelä, M.; Kinnunen, P. K. J. *Biochim. Biophys. Acta, Biomembr.* **2014**, *1838*, 1344.

(23) Kim, Y.-G.; Sohn, E. J.; Seo, J.; Lee, K.-J.; Lee, H.-S.; Hwang, I.; Whiteway, M.; Sacher, M.; Oh, B.-H. *Nat. Struct. Mol. Biol.* **2005**, *12*, 38.

(24) Meier, C.; Aricescu, A. R.; Assenberg, R.; Aplin, R. T.; Gilbert, R. J. C.; Grimes, J. M.; Stuart, D. I. *Structure* **2006**, *14*, 1157.

(25) Kates, M.; Syz, J. Y.; Gosser, D.; Haines, T. H. *Lipids* **1993**, *28*, 877.

(26) Malyshka, D.; Pandiscia, L. A.; Schweitzer-Stenner, R. *Vib. Spectrosc.* **2014**, *75*, 86.

(27) Kooijman, E. E.; Swim, L. A.; Graber, Z. T.; Tyurina, Y. Y.; Bayır, H.; Kagan, V. E. *Biochim. Biophys. Acta, Biomembr.* **2017**, *1859*, 61.

(28) Hanske, J.; Toffey, J. R.; Morenz, A. M.; Bonilla, A. J.; Schiavoni, K. H.; Pletneva, E. V. *Proc. Natl. Acad. Sci. U. S. A.* **2012**, *109*, 125.

(29) Pandiscia, L. A.; Schweitzer-Stenner, R. *J. Phys. Chem. B* **2015**, *119*, 12846.

(30) Pandiscia, L. A.; Schweitzer-Stenner, R. *J. Phys. Chem. B* **2015**, *119*, 1334.

(31) Hong, Y.; Muenzner, J.; Grimm, S. K.; Pletneva, E. V. *J. Am. Chem. Soc.* **2012**, *134*, 18713.

(32) Pandiscia, L. A.; Schweitzer-Stenner, R. *Chem. Commun.* **2014**, *50*, 3674.

(33) Basova, L. V.; Kurnikov, I. V.; Wang, L.; Ritov, V. B.; Belikova, N. A.; Vlasova, I. I.; Pacheco, A. A.; Winnica, D. E.; Peterson, J.; Bayir, H.; Waldeck, D. H.; Kagan, V. E. *Biochemistry* **2007**, *46*, 3423.

(34) Mandal, A.; Hoop, C. L.; DeLucia, M.; Kodali, R.; Kagan, V. E.; Ahn, J.; van der Wel, P. C. A. *Biophys. J.* **2015**, *109*, 1873.

(35) McClelland, L. J.; Mou, T.-C.; Jeakins-Cooley, M. E.; Sprang, S. R.; Bowler, B. E. *Proc. Natl. Acad. Sci. U. S. A.* **2014**, *111*, 6648.

(36) Wang, Z.; Matsuo, T.; Nagao, S.; Hirota, S. *Org. Biomol. Chem.* **2011**, *9*, 4766.

(37) Hirota, S.; Hattori, Y.; Nagao, S.; Taketa, M.; Komori, H.; Kamikubo, H.; Wang, Z.; Takahashi, I.; Negi, S.; Sugiura, Y.; Kataoka, M.; Higuchi, Y. *Proc. Natl. Acad. Sci. U. S. A.* **2010**, *107*, 12854.

(38) Hayashi, Y.; Nagao, S.; Osuka, H.; Komori, H.; Higuchi, Y.; Hirota, S. *Biochemistry* **2012**, *51*, 8608.

(39) Yamanaka, M.; Nagao, S.; Komori, H.; Higuchi, Y.; Hirota, S. *Protein Sci.* **2015**, *24*, 366.

(40) Nagao, S.; Ueda, M.; Osuka, H.; Komori, H.; Kamikubo, H.; Kataoka, M.; Higuchi, Y.; Hirota, S. *PLoS One* **2015**, *10*, e0123653.

(41) Schejter, A.; Glauser, S. C.; George, P.; Margoliash, E. *Biochim. Biophys. Acta, Spec. Sect. Enzymol. Subj.* **1963**, *73*, 641.

(42) Moore, G. R.; Pettigrew, G. W. *Cytochromes c: Evolutionary, Structural and Physicochemical Aspects*; Springer-Verlag: New York, NY, 1990.

(43) Bennett, M. J.; Sawaya, M. R.; Eisenberg, D. *Structure* **2006**, *14*, 811.

(44) Berghuis, A. M.; Brayer, G. D. *J. Mol. Biol.* **1992**, *223*, 959.

(45) Pattanaik, P.; Bethel, C. R.; Hujer, A. M.; Hujer, K. M.; Distler, A. M.; Taracila, M.; Anderson, V. E.; Fritsche, T. R.; Jones, R. N.; Pagadala, S. R. R.; van den Akker, F.; Buynak, J. D.; Bonomo, R. A. *J. Biol. Chem.* **2009**, *284*, 945.

(46) Nukaga, M.; Mayama, K.; Hujer, A. M.; Bonomo, R. A.; Knox, J. R. *J. Mol. Biol.* **2003**, *328*, 289.

(47) Wilderman, P. R.; Shah, M. B.; Liu, T.; Li, S.; Hsu, S.; Roberts, A. G.; Goodlett, D. R.; Zhang, Q.; Woods, V. L.; Stout, C. D.; Halpert, J. R. *J. Biol. Chem.* **2010**, *285*, 38602.

(48) Shah, M. B.; Jang, H.-H.; Wilderman, P. R.; Lee, D.; Li, S.; Zhang, Q.; Stout, C. D.; Halpert, J. R. *Biophys. Chem.* **2016**, *216*, 1.

(49) Hohoff, C.; Börchers, T.; Rüstow, B.; Spener, F.; van Tilbeurgh, H. *Biochemistry* **1999**, *38*, 12229.

(50) Sanson, B.; Wang, T.; Sun, J.; Wang, L.; Kaczocha, M.; Ojima, I.; Deutsch, D.; Li, H. *Acta Crystallogr., Sect. D: Biol. Crystallogr.* **2014**, *70*, 290.

(51) Armstrong, E. H.; Goswami, D.; Griffin, P. R.; Noy, N.; Ortlund, E. A. *J. Biol. Chem.* **2014**, *289*, 14941.

(52) Lee, C. W.; Kim, J. E.; Do, H.; Kim, R.-O.; Lee, S. G.; Park, H. H.; Chang, J. H.; Yim, J. H.; Park, H.; Kim, I.-C.; Lee, J. H. *Biochem. Biophys. Res. Commun.* **2015**, *465*, 12.

(53) Krishna, M. M.; Lin, Y.; Rumbley, J. N.; Englander, S. W. *J. Mol. Biol.* **2003**, *331*, 29.

(54) Duncan, M. G.; Williams, M. D.; Bowler, B. E. *Protein Sci.* **2009**, *18*, 1155.

(55) Kristinsson, R.; Bowler, B. E. *Biochemistry* **2005**, *44*, 2349.

(56) Amacher, J. F.; Zhong, F.; Lisi, G. P.; Zhu, M. Q.; Alden, S. L.; Hoke, K. R.; Madden, D. R.; Pletneva, E. V. *J. Am. Chem. Soc.* **2015**, *137*, 8435.

(57) Pangborn, M. C. *J. Biol. Chem.* **1947**, *168*, 351.

(58) Verdonk, M. L.; Cole, J. C.; Hartshorn, M. J.; Murray, C. W.; Taylor, R. D. *Proteins: Struct., Funct., Genet.* **2003**, *52*, 609.

(59) Kapralov, A. A.; Yanamala, N.; Tyurina, Y. Y.; Castro, L.; Samhan-Arias, A.; Vladimirov, Y. A.; Maeda, A.; Weitz, A. A.; Peterson, J.; Mylnikov, D.; Demicheli, V.; Tortora, V.; Klein-Seetharaman, J.; Radi, R.; Kagan, V. E. *Biochim. Biophys. Acta, Biomembr.* **2011**, *1808*, 2147.

(60) Vlasova, I. I.; Tyurin, V. A.; Kapralov, A. A.; Kurnikov, I. V.; Osipov, A. N.; Potapovich, M. V.; Stoyanovsky, D. A.; Kagan, V. E. *J. Biol. Chem.* **2006**, *281*, 14554.

(61) Gronenborn, A. M. *Curr. Opin. Struct. Biol.* **2009**, *19*, 39.

(62) Hayashi, Y.; Yamanaka, M.; Nagao, S.; Komori, H.; Higuchi, Y.; Hirota, S. *Sci. Rep.* **2016**, *6*, 19334.

(63) Herrmann, L. M.; Bowler, B. E. *Protein Sci.* **1997**, *6*, 657.

(64) Cohen, D. S.; Pielak, G. J. *Protein Sci.* **1994**, *3*, 1253.

(65) Parui, P. P.; Deshpande, M. S.; Nagao, S.; Kamikubo, H.; Komori, H.; Higuchi, Y.; Kataoka, M.; Hirota, S. *Biochemistry* **2013**, *52*, 8732.

(66) Deshpande, M. S.; Parui, P. P.; Kamikubo, H.; Yamanaka, M.; Nagao, S.; Komori, H.; Kataoka, M.; Higuchi, Y.; Hirota, S. *Biochemistry* **2014**, *53*, 4696.

(67) Liu, L.; Byeon, I.-J. L.; Bahar, I.; Gronenborn, A. M. *J. Am. Chem. Soc.* **2012**, *134*, 4229.

(68) Jerala, R.; Žerovnik, E. *J. Mol. Biol.* **1999**, *291*, 1079.

(69) Goldes, M. E.; Jeakins-Cooley, M. E.; McClelland, L. J.; Mou, T.-C.; Bowler, B. E. *J. Inorg. Biochem.* **2016**, *158*, 62.

(70) Laun, P.; Buettner, S.; Rinnerthaler, M.; Burhans, W. C.; Breitenbach, M. In *Subcellular Biochemistry: Aging Research in Yeast*; Breitenbach, M., Jazwinski, S. M., Laun, P., Eds.; Springer: Amsterdam, The Netherlands, 2012; Vol. 57, p 207.

(71) Cherney, M. M.; Junior, C.; Bowler, B. E. *Biochemistry* **2013**, *52*, 837.

(72) Pollock, W. B.; Rosell, F. I.; Twitchett, M. B.; Dumont, M. E.; Mauk, A. G. *Biochemistry* **1998**, *37*, 6124.

(73) Cutler, R. L.; Pielak, G. J.; Mauk, A. G.; Smith, M. *Protein Eng., Des. Sel.* **1987**, *1*, 95.

(74) Redzic, J. S.; Bowler, B. E. *Biochemistry* **2005**, *44*, 2900.

(75) Wandschneider, E.; Hammack, B. N.; Bowler, B. E. *Biochemistry* **2003**, *42*, 10659.

(76) Jones, G.; Willett, P.; Glen, R. C.; Leach, A. R.; Taylor, R. *J. Mol. Biol.* **1997**, *267*, 727.